

Self-assembly of isotropic colloids into colloidal strings, Bernal spiral-like, and tubular clusters

Yong Guo^{a*}, Bas G. P. van Ravensteijn^{b*} and Willem K. Kegel^c

^a School of Medicine, Hangzhou Normal University, Hangzhou 311121, People's Republic of China

^b Institute for Complex Molecular Systems, Eindhoven University of Technology, 5600 MD Eindhoven, The Netherlands

^c Van 't Hoff Laboratory for Physical and Colloid Chemistry, Debye Institute for NanoMaterials Science, Utrecht University, 3584 CH Utrecht, The Netherlands

CONTENTS

S1 Experimental section	2
S2 Importance of Van der Waals vs. hydrophobic attractions	4
S3 Homogeneity of the grafted brush	5
S4 Infrared spectra of CPS-Cl, CPS-C ₁₂ , and CPS-H ₁	6
S5 Effect of ionic strength on cluster morphology	7
S6 Additional optical microscopy images of tubular assemblies of CPS-H ₁	8

S1 Experimental section

S1.1 Materials. Styrene (St, 99%), divinylbenzene (DVB, 55% mixture of isomers, tech. grade), 4-vinylbenzyl chloride (VBC, $\geq 90\%$, tech. grade), dimethylformamide (DMF, $\geq 99\%$), acetonitrile (ACN, GC, $\geq 99.5\%$), fluorescein sodium salt, *t*-butyl acrylate (*t*BA, 98%), copper(I) bromide (Cu(I)Br, 98%), 2,2'-bipyridyl (Bpy, ReagentPlus, 99%), *n*-butylamine (Bu-NH₂, 99.5%), and *N,N*-dimethyldodecylamine (DMDA, 97%) were obtained from Sigma-Aldrich. Sodium dodecyl sulfate (SDS) from BDH was used. Sodium bisulfite (NaHSO₃, ACS reagent) and potassium persulfate (KPS, $> 99\%$ for analysis) were purchased from Acros Organics. Ethanol (p.a., ACS reagent) was purchased from Merck. Methanol (exceeds ACS specifications) was obtained from J.T. Baker. Triethylamine (TEA, puriss. p.a.; $\geq 99.5\%$) was obtained from Fluka. All chemicals were used as received. The water used throughout all of the synthesis was purified using a Milli-Q purification system.

S1.2 Synthesis of negatively charged chlorinated polystyrene colloids (CPS-Cl). CPS-Cl were synthesized by seeded emulsion polymerization as described in Reference S1. The CPS-Cl have a zeta (ζ) potential of -38 mV.

S1.3 Synthesis of triethylamine functionalized colloids (CPS-C₂). TEA (35 μ L, 0.25 mmol) was injected into an aqueous CPS-Cl dispersion (1 mL, solid content = 1%). The mixture was stirred for 24 h at room temperature. The product was washed three times with ethanol and water sequentially, and finally the particles were dispersed and stored in water. The CPS-C₂ have a ζ potential of 47 mV.

S1.4 Synthesis of *n*-butylamine functionalized colloids (CPS-C₄). Bu-NH₂ (100 μ L, 1 mmol) was added into an ethanolic CPS-Cl dispersion (1 mL, solid content = 1%). The mixture was stirred for 24 h at room temperature. The product was washed three times with ethanol and water sequentially, and finally the particles were dispersed and stored in water. The CPS-C₄ have a ζ potential of 50 mV.

S1.5 Synthesis of *N,N*-dimethyldodecylamine functionalized colloids (CPS-C₁₂). DMDA (200 μ L, 0.7 mmol) was added into an ethanolic CPS-Cl dispersion (2 mL, solid content = 1%). The mixture was stirred for 24 h at room temperature. During the reaction, aliquots (100 μ L) were withdrawn from the reaction mixture after 5, 45, 60, 90, 150, 180, and 480 min. The samples were washed three times with ethanol and water sequentially, and finally the particles were dispersed and stored in water. The CPS-C₁₂ have a ζ potential of 46 mV.

S1.6 Synthesis of poly(*t*-butyl acrylate) grafted colloids (CPS-H₁). Bpy (14 mg, 0.09 mmol) and Cu(I)Br (6.5 mg, 0.045 mmol) were added in a 10 mL, oven-dried Schlenk flask. The flask was degassed by evacuation and refilling with nitrogen three times. In another oven-dried Schlenk flask, DMF (1 mL) and *t*BA (73 μ L, 0.5 mmol) were added and oxygen was excluded from the reaction flask following the same degassing procedure as mentioned before. The degassed monomer solution was quickly transferred into the flask containing the copper based catalytic system, followed by an additional degassing cycle. Subsequently, degassed CPS-Cl dispersion in DMF (1 mL, solid content = 1%) was injected into the monomer and catalyst containing flask. Upon mixing, the mixture became dark brown. After a final degassing cycle, the reaction flask was placed in a 90 °C oil bath where the ATRP reaction was allowed to continue for 24 h under constant stirring. The polymerization was quenched by exposing the dispersion to air. The product was washed several times with methanol, 50 mM aqueous NaHSO₃ solution and water sequentially. Finally, the particles were dispersed and stored in water. The CPS-H₁ have a ζ potential of 30 mV.

S1.7 Synthesis of poly(*tert*-butyl acrylate) grafted colloids (CPS-H₂). The synthesis procedure of CPS-H₂ is essentially the same as described for CPS-H₁ (subsection S1.6), except that the acetonitrile/water mixture (v/v = 8:2) was used as solvent system. Additionally, the reaction temperature was kept at 60 °C to minimize the evaporation of acetonitrile. The CPS-H₂ have a ζ potential of -31 mV.

S1.8 Assembly of hydrophobically modified colloids into elongated clusters. Typically, an aqueous colloidal dispersion (volume fraction \approx 0.5%) was sonicated for approximately 30 min to disintegrate any clusters and ensure a homogeneous dispersion of well-dispersed particles as starting point. Subsequently, the colloidal dispersion was kept at rest for one week. After spontaneous particle sedimentation, the colloids/clusters were gently redispersed by manual shaking. Alternatively, to speed up the self-assembly process, the sample was centrifuged at 2100g for 2 h. After centrifugation, the colloids and/or clusters were gently redispersed by manual shaking. The physical appearance of the dispersion was investigated using optical microscopy. To this end, 5 μ L of the dispersion was placed on a home-made microscopy cell (for details see Section S1.9).

S1.9 Characterization. Transmission electron microscopy (TEM) pictures were taken with a Philips Tecnai 10 electron microscope typically operating at 100 kV. The samples were prepared by drying a drop of diluted aqueous dispersion on top of polymer-coated copper grids.

Scanning electron microscopy (SEM) images were taken with a Philips SEM XL FEG 30 typically operating at 5 – 10 kV. In order to freeze-dry SEM samples, 1 μ L dispersion was brought on a polymer coated copper grid. The grid was vitrified in liquid nitrogen and mounted onto a cryo transfer unit which was brought under vacuum of 10^{-4} Pa. The temperature was increased to -90 °C at 5 °C/min and kept constant for approximately 6 h under vacuum to allow the water to sublime. The freeze-dried samples were sputter coated with 6 nm platinum prior to imaging.

Infrared (IR) spectra were obtained using a PerkinElmer Frontier FT-IR/FIR spectrometer. The attenuated total reflectance (ATR) mode was used. Measurements were performed on powders obtained by drying the particles dispersion. All the IR spectra were normalized with respect to a polystyrene related signal (695 cm^{-1}).

Optical microscopy (OM) images were taken with a Nikon Ti-E inverted microscope. The microscope was equipped with a Nikon TIRF NA 1.49 100 \times oil immersion objective, intermediate magnification of 1.5 \times , and a Hamamatsu ORCA Flash camera. Dedicated microscopy cells were fabricated for particle/cluster imaging. To this end, two coverslip glasses (VWR, #0, 22 \times 22 mm) were placed at a distance of approximately 15 mm from each other on a microscope slide (Menzel-Gläser) and fixated with tape. Subsequently, a drop of dispersion was injected in between the coverslips. The sample cell was then closed by taping an additional coverslip (Menzel-Gläser, #1.5, 22 \times 22 mm) on top of the two immobilized coverslips. All used glass slides were cleaned with water and ethanol and dried with Kimtech precision wipes before use. The colloidal dispersions were monitored through the coverslip side of the sample cell.

Zeta (ζ) potentials were determined by laser Doppler electrophoresis. The radii of particles (R) were approximately 200 nm, while the Debye length (κ^{-1}) is on the order of 100 nm under the conditions at which the electrophoresis measurements were conducted (Milli-Q water). Hence, $\kappa R > 1$, justifying the use of the Smoluchowski limit of the Henry equation to convert the measured electrophoretic mobilities into the reported ζ potentials.^{S2}

S2 Importance of Van der Waals vs. hydrophobic attractions

Judging from the observation that colloidal stability was regained after charge reversal implies that the particles are not trapped in deep attractive (van der Waals) potential well close to the isoelectric point. This was previously ascribed to the rough particle surface which provides a limit to the minimal interparticle distance and therefore, to the magnitude of the van der Waals attraction.^{S3} Hence, we speculate that the hydrophobic interactions originating from the immobilized aliphatic amines are the dominating driving force for assembly after/during grafting of the aliphatic amines.

S3 Homogeneity of the grafted brush

To strengthen our claim that the particles are homogeneously grafted and therefore interact via isotropic inter-particle potentials, we tried to assess the uniformity of our particle surfaces. In the case of colloids grafted with small hydrophobic molecules (CPS- C_n), direct visualization of the homogeneity of the hydrophobic layer by, for example, AFM, TEM or SEM is not possible, since the layer has only molecular thicknesses and is therefore extremely small compared to the roughness of the particle surface. Alternatively, the distribution of the chlorine groups was probed using confocal microscopy after covalent attachment of fluorescein amine.^{S1} As shown in Figure S1a, the fluorescence is homogeneously distributed over the particle surface on the probed length scale, indicating a uniform coverage of the particle surface with reactive chlorines. This uniform distribution will translate to a homogeneous grafting of the aliphatic amines.

For CPS- H_1 and CPS- H_2 , which carry thicker grafted layers on their surface, we performed transmission electron microscopy (TEM) analysis to analyze the surface features of the colloids. A representative TEM image of CPS- H_2 is shown in Figure S1b. Clearly, the particles appear to have a homogeneous surface morphology without patch formation that could indicate an asymmetric distribution of polymers. Therefore, we concluded that the grafted layer is homogenous, as is the potential acting between these colloids.

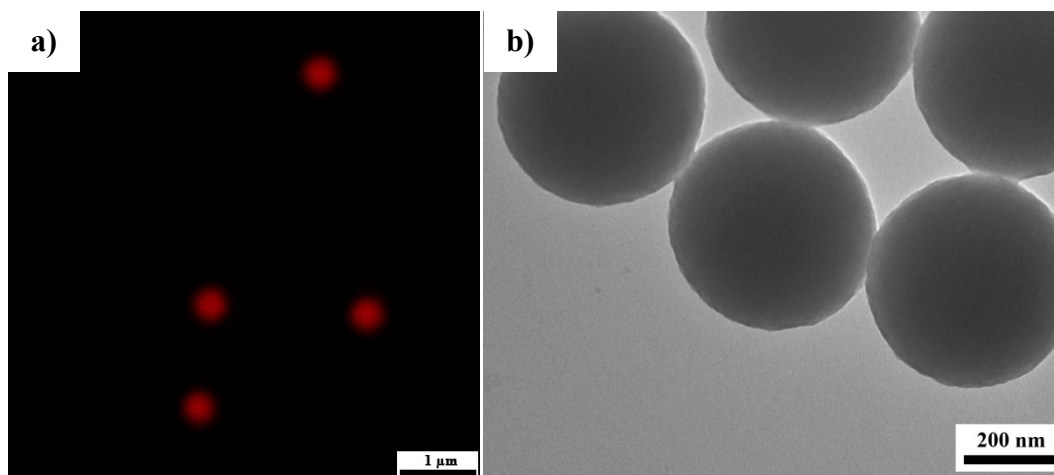


Figure S1. Confocal microscope image of dye functionalized CPS-Cl and TEM image of CPS- H_2 .

S4 Infrared spectra of CPS-Cl, CPS-C₁₂, and CPS-H₁

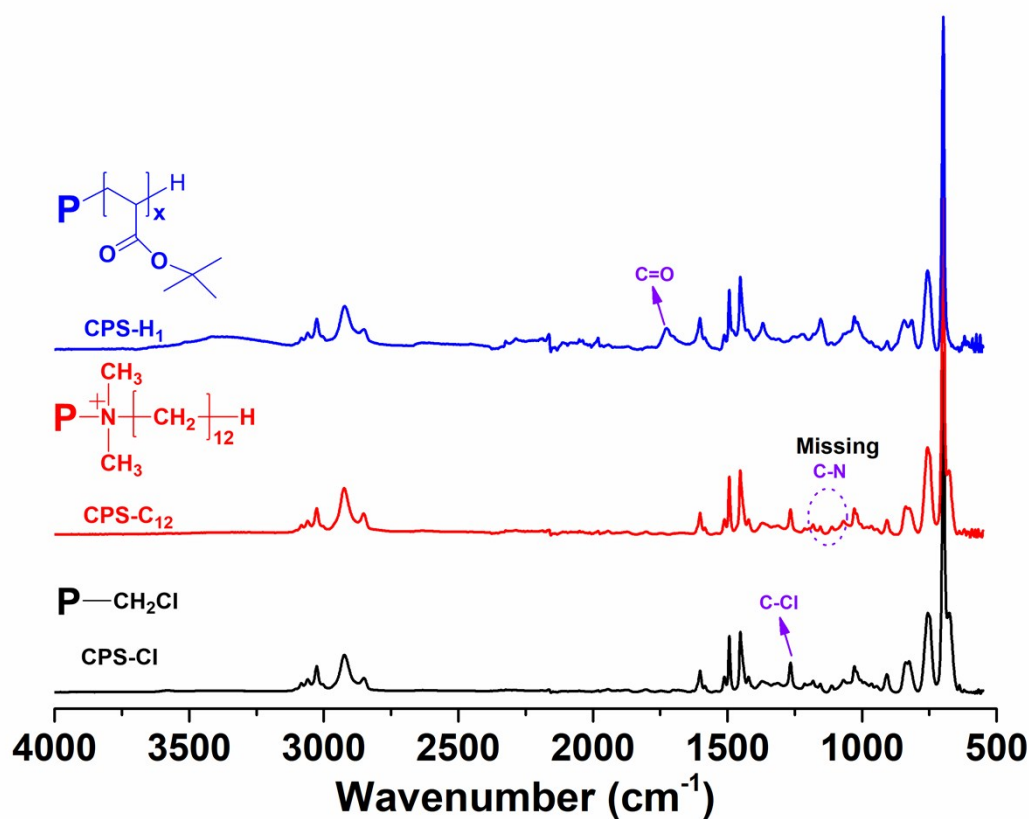


Figure S2. Infrared spectra of the chlorinated colloids (CPS-Cl), the *N,N*-dimethyldodecylamine modified colloids (CPS-C₁₂), and the poly(*t*-butyl acrylate) (p(*t*BA)) grafted colloids (CPS-H₁). The presence of a carbonyl (C=O) stretching vibration in the spectra of CPS-H₁ indicates p(*t*BA) chains were indeed grafted to the colloidal surface. However, in the case of CPS-C₁₂, the absence of any diagnostic C-N vibration implies the introduced amines were undetectable with IR spectroscopy and the recorded spectrum is completely dominated by the polystyrene bulk of the particles.

S5 Effect of ionic strength on cluster morphology

To gain more insight into the influence of the electrostatic repulsion, the ionic strength of a dispersion containing CPS-C₄ was raised from approximately 0.01 mM (Milli-Q water) to 2 mM by addition of NaCl. The raise in ionic strength induces a decrease of electrostatic repulsion, which eventually results in a morphological transition of the colloidal strings into more compact spherical aggregates (Fig. S3). Although the colloidal string is most likely not an equilibrium structure, we note that this transition is consistent with simulation studies of Mossa et al., where the presence of elongated structures was only observed when the repulsive contribution to the interparticle potential is sufficiently high. Despite that their interaction range was significantly higher than the range in our system, a transition to predominantly spherical structures was found when diminishing the repulsive term.^{S4}

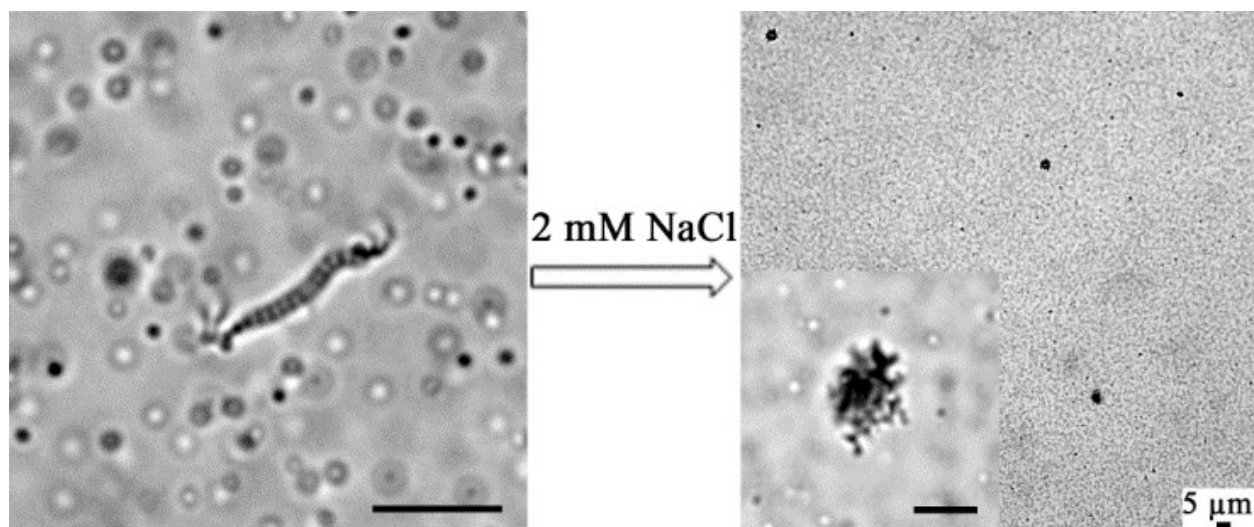


Figure S3. Optical micrographs of *n*-butylamine modified CPS-Cl (CPS-C₄) in (left) Milli-Q water and (right) 2 mM aqueous NaCl solution. Scale bars: 5 μm for all images.

S6 Additional optical microscopy images of tubular assemblies of CPS-H₁

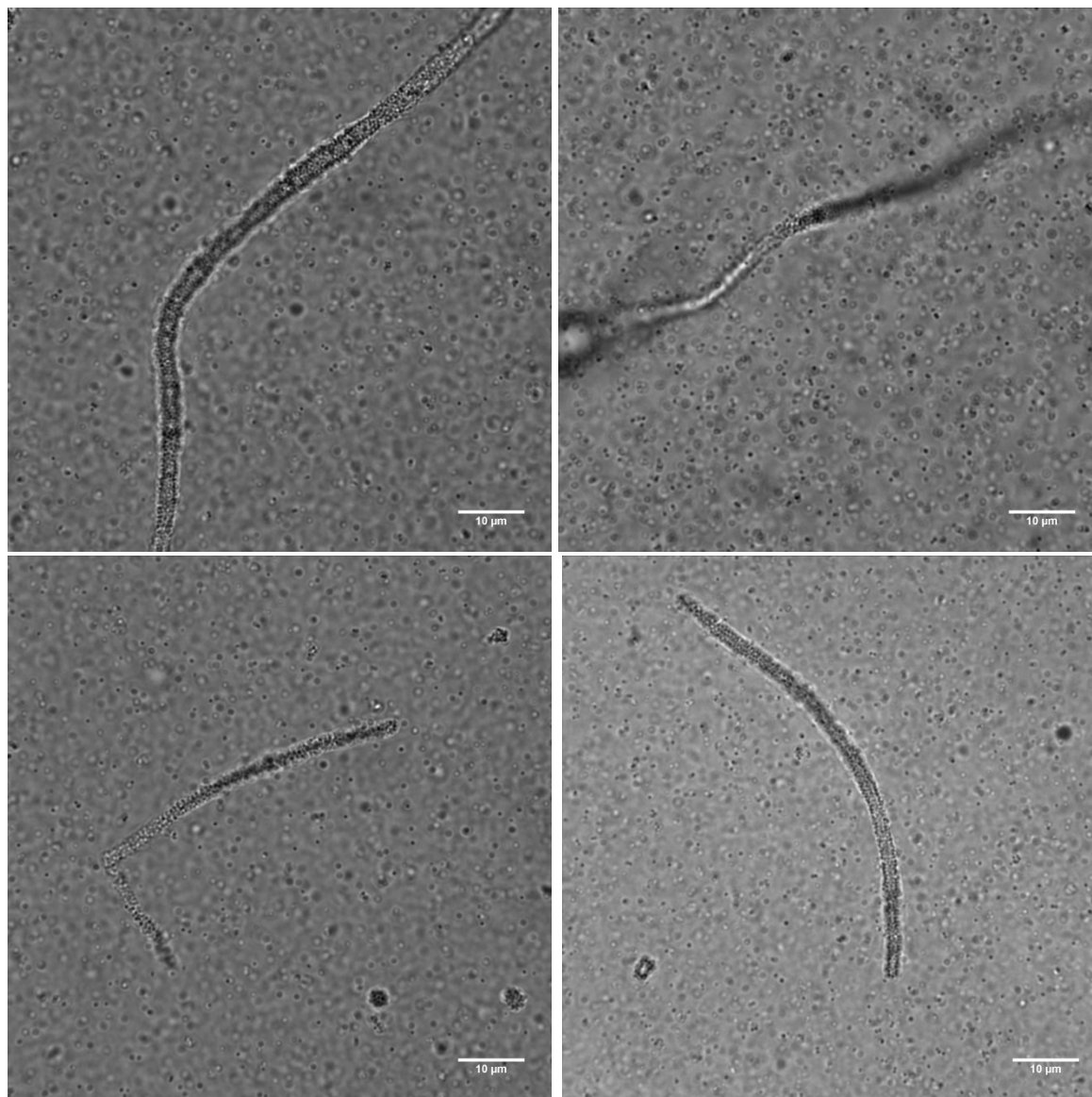


Figure S4. Additional optical microscopy images of tubular assemblies of CPS-H₁. Scale bar: 10 μm.

References

- S1. van Ravensteijn, B. G. P.; Kamp, M.; van Blaaderen, A.; Kegel, W. K., General Route toward Chemically Anisotropic Colloids. *Chem. Mater.* **2013**, 25 (21), 4348-4353.
- S2. Hunter, R. J., *Zeta Potential in Colloid Science*. Academic Press: 1981.
- S3. van Ravensteijn, B. G. P.; Kegel, W. K., Colloids with Continuously Tunable Surface Charge. *Langmuir* **2014**, 30 (35), 10590-10599.
- S4. Mossa, S.; Sciortino, F.; Tartaglia, P.; Zaccarelli, E., Ground-State Clusters for Short-Range Attractive and Long-Range Repulsive Potentials. *Langmuir* **2004**, 20 (24), 10756-10763.